Electronic Supplementary Information†

Switchable Molecular Electrocatalysis

Shifali Dutt[a‡], Alagar Raja Kottaichamy[a,d‡], Neethu Christudas Dargily[a‡], Sanchayita Mukhopadhyay[a], Bhojkumar Nayak[a], Mruthyunjayachari Chattanhali Devendrachari[a], Chatakudhath Prabakaran Vinod[b], Harish Makri Nimbegondi Kotresh[c], Musthafa Ottakam Thotiyl[a]*

[a] Shifali Dutt‡, Alagar Raja Kottaichamy‡, Neethu Christudas Dargily‡, Sanchayita Mukhopadhyay, Bhojkumar Nayak, Mruthyunjayachari Chattanhali Devendrachari, Musthafa Ottakam Thotiyl*
Indian Institute of Science Education and Research (IISER) Pune, Dr. Homi Bhabha Road, Pashan, Pune, 411008, India
Email: musthafa@iiserpune.ac.in

[b] Chatakudhath Prabakaran Vinod
Catalysis and Inorganic Division, CSIR-NCL, Pune 411008, India

[c] Harish Makri Nimbegondi Kotresh
Department of Chemistry, Acharya Institute of Technology, Soldevanahalli, Bangalore-560107, India

[d] Department of Chemistry, Ilse Katz Institute for Nanoscale Science and Technology, Ben-Gurion University of the Negev, Beer-Sheva 8410501, Israel

‡ These authors contributed equally

Table of Contents

1. Materials and Methods

1.1 Chemicals: Chemicals including cobalt (II) chloride hexahydrate (≥98 %), zinc (II) chloride hydrate ($ZnCl_2$, 99.99 %), 4-nitrophthalimide (98 %), 3-nitrophthalimide (98 %), sodium sulfide nonahydrate (≥98 %), ammonium molybdate (99.99 %), ammonium chloride (≥98 %), nitrobenzene (99 %), toluene (99.5 %), methanol (99%), ethanol (95 %), N,N dimethylformamide (DMF, 99 %), hexane (95 %), isopropyl alcohol (99 %), and sulfuric acid (96 %) were procured from Alfa Aesar, India. Dimethyl sulfoxide-d6 (DMSO-d6, 99.9 % atom D), hydrochloric acid (37.0 wt %), and Nafion solutions (5 wt %) were obtained from Sigma-Aldrich, India.

1.2 Electrochemical measurements: Electrochemical tests were conducted using a Biologic potentiostat in a typical three-electrode cell comprising a 2 mm diameter gold disc as the working electrode, Ag/AgCl (3 M KCl) as the reference electrode, and Pt mesh as the counter electrode. Millipore water (18.2 MΩ.cm) was utilized for solution preparation, and a constant cell temperature of 25 °C was maintained. Tafel slope measurements were performed employing steady-state polarization in the electron transfer limiting area. Redox potentials for hydrogen redox reactions in the corresponding electrolytes were determined using a Pt disc working electrode, ultimately converted to the reversible hydrogen scale (RHE scale). For oxygen reduction reaction and hydrogen evolution reactions, experiments were also repeated with a graphite counter electrode. Since the results were found to be the same irrespective of the counter electrode, the data with only Pt counter is provided in this investigation.

1.3 Characterization techniques: Ultraviolet-visible (UV-vis) spectroscopy using a Perkin Elmer Lambda 950 instrument, Fourier-transform infrared (FTIR) spectroscopy employing a Bruker Alpha attenuated total reflectance FTIR spectrometer, morphological characterizations and elemental analysis utilizing a scanning electron microscope (SEM) fitted with an energy-dispersive X-ray spectroscopy (EDS) detector (Zeiss Ultraplus-4095), Raman spectra captured using a Raman microscope (LabRAM HR, Horiba Jobin Yvon), nuclear magnetic resonance (NMR) spectra obtained using a Bruker 400 MHz spectrometer, and X-ray photoelectron spectroscopy (XPS) conducted using a Thermo Scientific Kalpha+ spectrometer were employed. Avantage software (Thermo Fisher Scientific) was utilized for peak fitting, ensuring a 2:1 ratio of $2p_{3/2}$ and $2p_{1/2}$ in Co 2p during peak fitting. Raman experiments were carried out with an excitation wavelength of 785 nm with an output power ≈ 170mV. EPR was recorded using an EMX micro–X BRUKER EPR Spectrometer with an X band on solid samples

2. Experimental Section: Synthesis Protocol for α/β TNCoPc and α/β TACoPc

Cobalt tetraminophthalocyanine (1,8,15,22-tetraaminophthalocyanatocobalt (II) (α TACoPc), 2,9,16,23 tetraaminophthalocyanatocobalt(II) (β TACoPc)), Cobalt tetranitro phthalocyanine (1,8,15,22-tetranitrophthalocyanatocobalt(II) (α TNCoPc) and 2,9,16,23 tetranitrophthalocyanatocobalt(II) (β TNCoPc)) were synthesized following literature procedures.[1]

2.1 Synthesis of 2,9,16,23-Tetranitro Co Phthalocyanine / 1,8,15,22- Tetranitro Co Phthalocyanine: A mixture of 4-nitro phthalimide / 3-nitro phthalimide, urea, ammonium molybdate, ammonium chloride, and nitrobenzene was stirred and heated, followed by refluxing. The resulting solid was filtered, washed, and dried.

2.2. Preparation of 2,9,16,23-Tetraaminophthalocyanatocobalt (II) / 1,8,15,22Tetraamino phthalocyanatocobalt(II) from 2,9,16,23-Tetranitrophthalocyanatocobalt(II) / 1,8,15,22-Tetranitrophthalocyanatcobalt(II): A mixture of tetra nitro Cobalt Phthalocyanine, sodium sulphide nonhydrate, and N,N, dimethyl formamide underwent heating, cooling, and filtration, yielding the desired compounds.

2.3 Synthesis of 2,9,16,23-Tetraaminophthalocyanatocobalt (II) / 1,8,15,22Tetraamino phthalocyanatocobalt(II) incorporated over CNT : Separately, α- and β-TACoPc were combined with carbon nanotubes (CNT) in DMF at a stoichiometric ratio of 3:7 (w/w). Subsequently, the blend underwent a 30-minute sonication. The suspension was agitated for 24 hours at 80°C following sonication. The final precipitate was obtained by centrifuging the mixture, and it was then thoroughly washed with DMF and then ethanol. The washed precipitate was dried overnight at 65°C in the vacuum oven to produce the final composite.[2]

3. Fabrication of Nanoporous Gold Electrodes (NPG Au):

Prior to surface modification, the Au electrode underwent thorough polishing using alumina slurry. Subsequently, the gold electrode was subjected to polarization from 0.0 to 2.0 V at a scan rate of 20 mV/s in a 0.5 M H_2SO_4 solution. Following the forward scan, the gold electrode potential was maintained at 2.0 V vs. Ag/AgCl (3M KCl) for 20 minutes, leading to the formation of a gold oxide film with an orange-yellowish hue on the electrode surface. The selection of 2.0 V, slightly higher than the threshold for gas evolution, aimed to ensure the uniform structure and stability of the NPG Au electrode, as higher potentials risked the evolution of gas bubbles onto the electrode surface, potentially affecting nanoporous structure formation and stability. Subsequently, the generated oxide layer was reduced during the reverse scan, resulting in the formation of a nanoporous gold film with a grey coloration, as depicted in Fig. S2a.

4. Self-assembly of α TACoPc and β TACoPc on Au and NPs Au electrodes:

Mono layer assembly of α and β TACoPc molecules on the electrode surfaces was accomplished through a self-assembly process. Solutions of 6 mM α and β TACoPc were prepared in dimethyl formamide (DMF) via ultrasonication. Flat Au electrodes underwent initial polishing with alumina polishing powder followed by electrochemical cleaning. Electrochemical cleaning involved cycling between potentials of -0.2 to 1.6 V in 0.1 M H_2SO_4 until reproducible voltammograms were obtained. The electrodes were thoroughly rinsed with distilled water and DMF. Both flat Au electrodes and NPG Au electrodes were immersed in 6 mM α and β TACoPc solutions for 24 hours. Subsequently, the modified electrodes were washed with fresh DMF to remove physisorbed molecules and finally rinsed with distilled water.

5. Calculation of the number of electron and H_2O_2 % yield for ORR

Rotating ring disk electrode (RRDE) experiments were carried out using PINE instruments in conjunction with a PARSTAT MC (AMETEK) potentiostat. Glassy carbon (GC) disk electrodes (with an area of 0.196 cm^2) and platinum (Pt) ring electrodes (with an area of 0.11 cm^2) were utilized in these experiments. The electrodes underwent cleaning by immersion in a diluted solution of hydrogen peroxide and sulfuric acid, followed by thorough rinsing in boiling water and subsequent electrochemical cleaning in 0.1 M H_2SO_4 solution within the potential range of 0.2 to 1.3 V vs. RHE. The disk electrode was then modified by drop-casting with α -TACoPc and β- TACoPc. Catalyst ink preparation involved sonicating a specific quantity of catalyst in 2-propanol (IPA) with 5 wt % PVDF as the binder to achieve a homogeneous dispersion.

All RRDE electrochemical measurements were performed in a 0.1 M H_2SO_4 solution saturated with oxygen, employing a three-electrode configuration consisting of a glassy carbon electrode modified with α -TACoPc or β -TACoPc. The disk electrode underwent cathodic scanning from 0.85 to –0.15 V vs. RHE at a scan rate of 5 mV s^{-1}, while the ring potential was maintained constant at 1.0 V vs. RHE. Disk and ring currents were recorded at various rotation rates (100, 400, 900, 1600, 2500, and 3600 rpm). The H_2O_2 yield (% H_2O_2) and electron transfer number (n) were determined using equations S1 and S2, respectively.[3]

$$\% \, \mathrm{H_2O_2} = 200 \left[\left(\frac{I_\mathrm{r}}{N} \right) / \left(I_\mathrm{d} + \left(\frac{I_\mathrm{r}}{N} \right) \right) \right] \qquad \text{(S1)}$$

$$n = 4 \left[I_\mathrm{d} / \left(I_\mathrm{d} + \left(\frac{I_\mathrm{r}}{N} \right) \right) \right] \qquad \text{(S2)}$$

The determination of the collection efficiency, denoted as N with a value of 0.37 was deduced from RRDE profiles of Ar-saturated 10 mM potassium ferricyanide solution at 1600 RPM.

6. In-situ electrochemical Raman spectroscopy:

In-situ electrochemical Raman spectra of the β /α-TACoPc was carried out with self-assembled monolayer (SAM) on gold foil as working electrode, assembled in EL-Raman-Opto Cell (ECC-Opto-Std-Aqu) with gold reference and counter electrodes, enabling Raman analysis in the reflective mode. In-situ electrochemical Raman spectroscopic analysis of β /α isomer in a 0.1 M H_2SO_4 solution saturated with oxygen spanning from 1 V to 0.3 V vs. RHE for ORR and 0.16 V to -0.38 V vs RHE for HER with a scan rate of 1 mV/s, collecting Raman spectrum at every 25 sec.

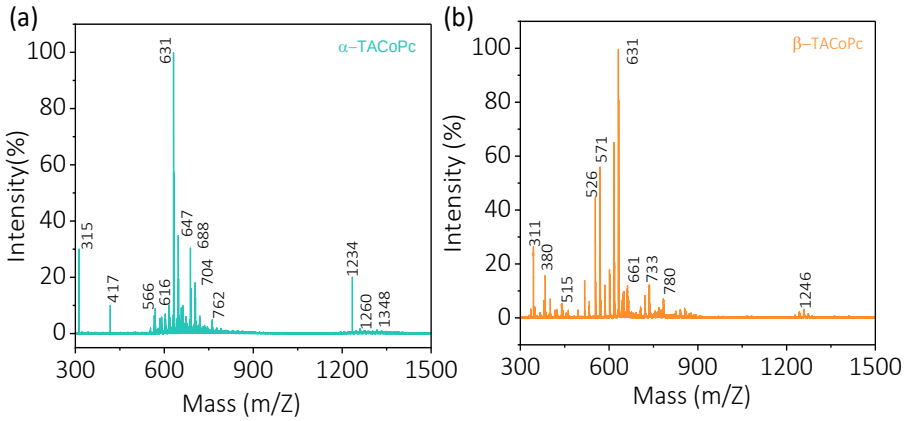

Figure S1: MALDI-TOF data for (a) α-TACoPc and (b) β-TACoPc molecules.

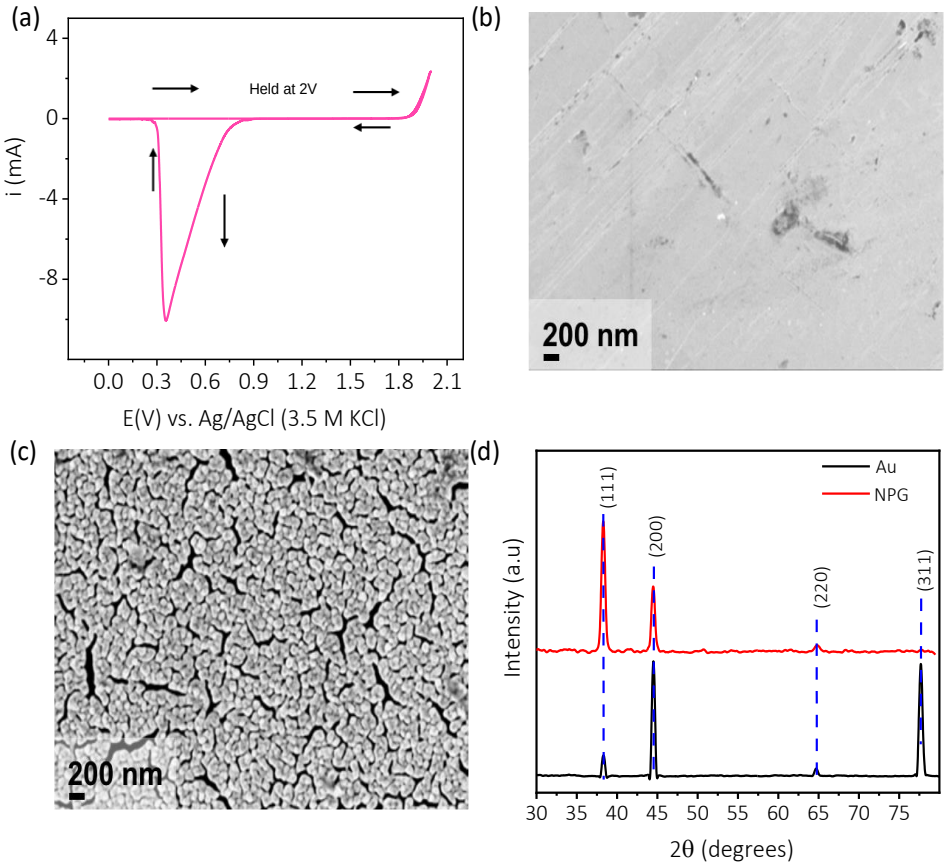

Figure S2: (a) Fabrication of the NPG-Au electrode in N_2 saturated 0.5 M H_2SO_4 at a scan rate of 20 mV/s by holding the potential for 20 minutes. (b, c) FESEM images of bare Au and NPG electrode surface respectively. (d) X-ray diffraction pattern of bare Au (black trace) and NPG (red trace)

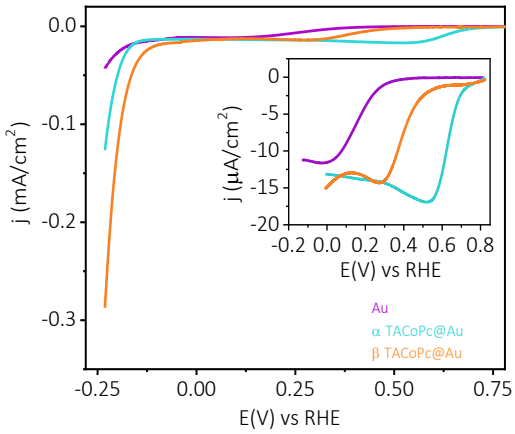

Figure S3: Simultaneous voltammograms of monolayer modified Au electrodes with α -TACoPc and β -TACoPc isomer molecules in oxygen saturated 0.1 M H_2SO_4 electrolyte at a scan rate of 5 mV/s

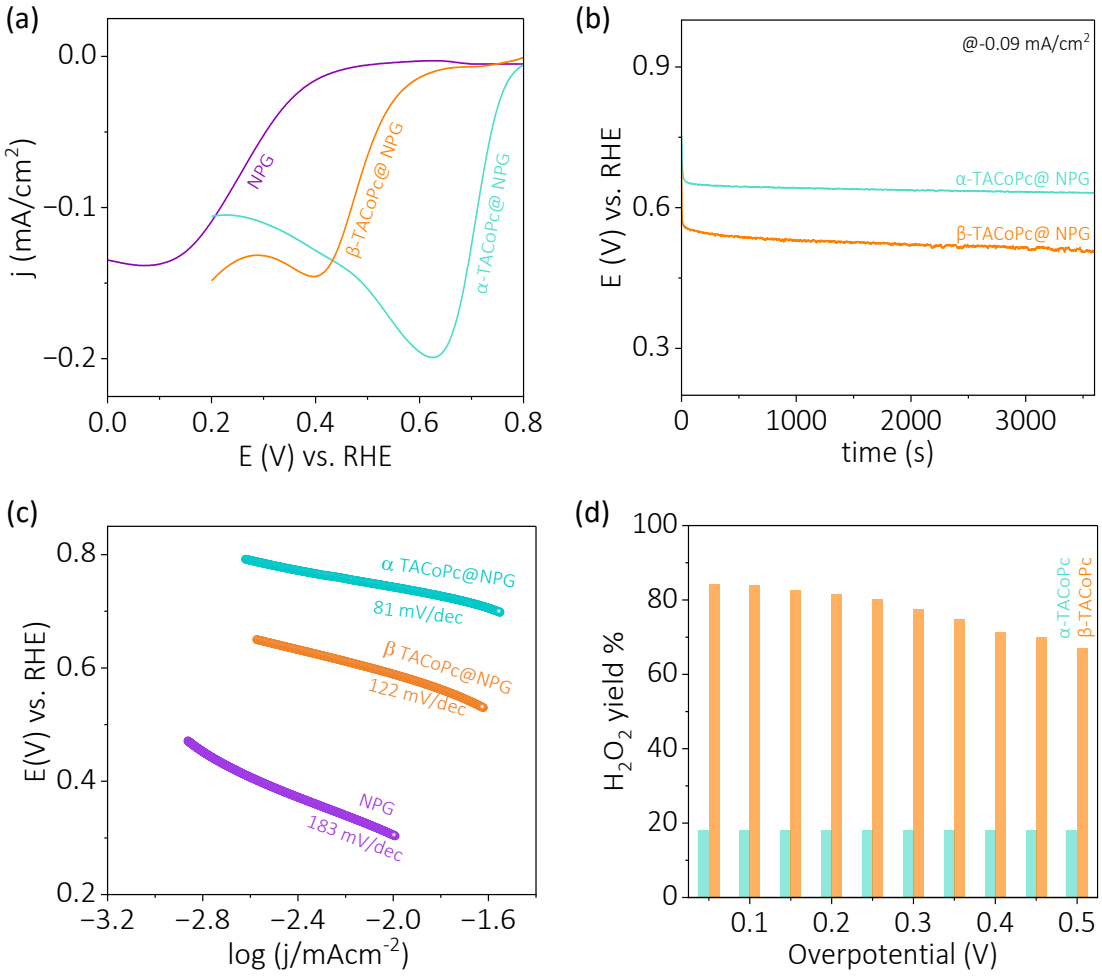

Figure S4: a) Voltammograms of α-TACoPc and β-TACoPc modified NPG electrodes in oxygen saturated 0.1 M H_2SO_4 electrolyte at a scan rate of 20 mV/s. b) Chronopotentiometry of α-TACoPc and β-TACoPc isomers in oxygen saturated 0.1 M H_2SO_4 electrolyte at -0.09 mA/cm^2.

c) Tafel plots of α-TACoPc and β-TACoPc modified NPG electrodes in oxygen saturated 0.1 M H_2SO_4 at 5mV/s d) H_2O_2 percentage with α-TACoPc and β-TACoPc electrodes in oxygen saturated 0.1 M H_2SO_4.

Table S1: Parameter extracted from Fig.S4a.

Type of electrodes	ORR	
	Onset potential (V vs. RHE)	Peak current (mA/cm^2)
NPG	0.44	0.13
α -TACoPc@NPG	0.79	0.21
β -TACoPc@NPG	0.63	0.15

Table S2: Tafel slope values extracted from Fig. S4c

Type of electrodes	Tafel slope (mV/dec) (ORR)
NPG	183
α -TACoPc@NPG	81
β - TACoPc@NPG	122

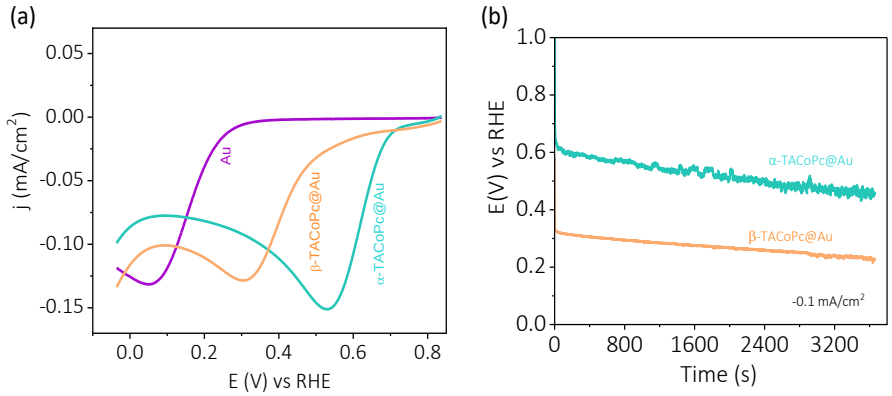

Figure S5: (a) Voltammograms of SAM modified Au electrode with α and β TACoPc molecules in 0.1 M H_2SO_4 electrolyte saturated with oxygen at a scan rate of 20 mV/s. (b) Chronopotentiometry at a current density of -0.1 mA/cm^2.

Table S3: Parameter calculated from Fig. S5a.

Type of electrodes	ORR	
	Onset potential (V vs. RHE)	Peak current (mA/cm^2)
Au	0.26	-0.12
α- TACoPc@Au	0.71	-0.15
β -TACoPc@Au	0.50	-0.13

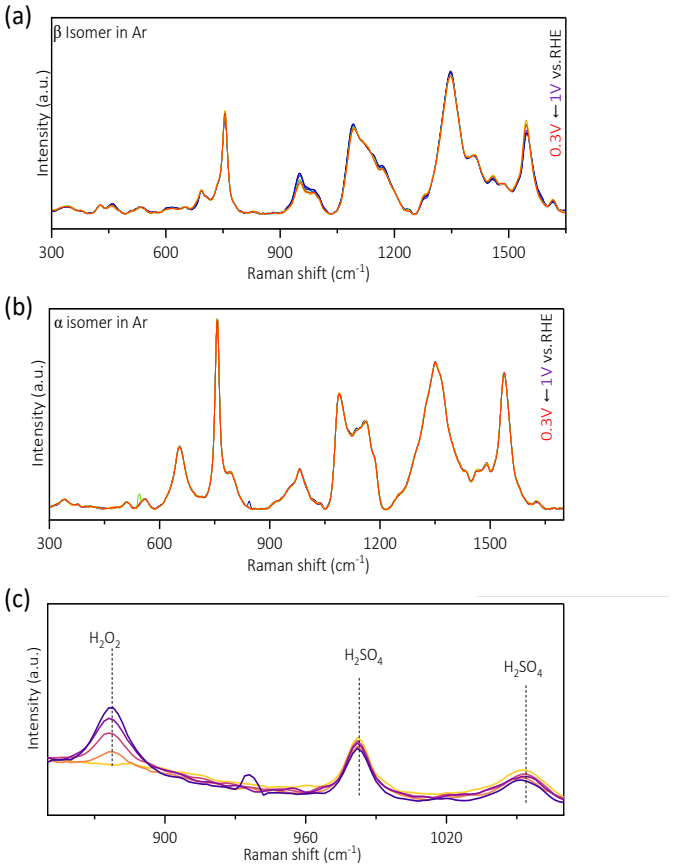

Figure S6: In situ raman spectra collected in argon atmosphere from 1V to -0.3V vs. RHE for (a) β TACoPc b) α TACoPc (c) Intensity change for varying concentration of H_2O_2 in 0.1M H_2SO_4,

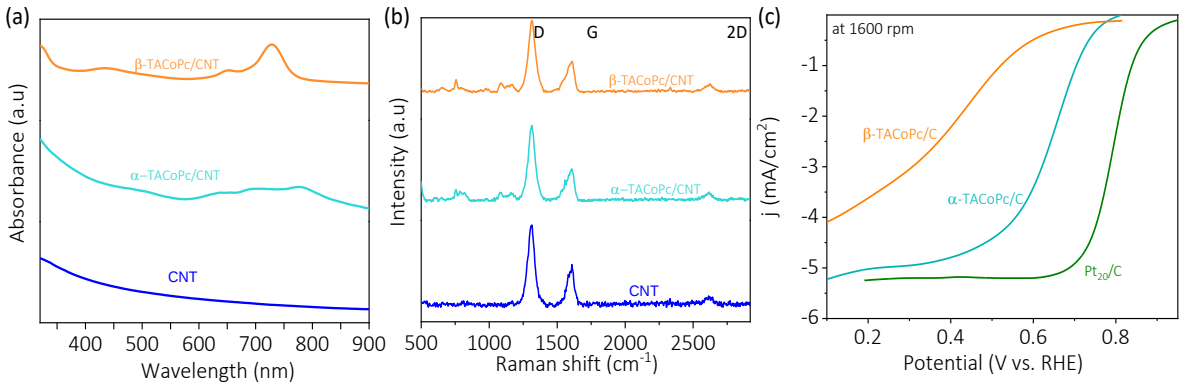

Figure S7: Characterization of α, and β-TACoPc isomer composites with CNT. a) UV-Vis spectra and b) Raman spectra. Electrochemical ORR activity of α, and β-TACoPc isomer composites with CNT and Pt/C (20 wt % of Pt) in oxygen saturated 0.1 M H_2SO_4 electrolytes at 1600 rpm.

Table S4: Electrochemical ORR activity of α and β-TACoPc isomer composites with CNT and Pt/C (20 wt% of Pt) in oxygen saturated 0.1 M H_2SO_4 (extracted from Fig. S7).

Type of electrodes	ORR performance metrics	
	Onset potential (V vs. RHE)	Current density at 0.3 V (mA/cm^2)
Pt/C	0.9	-5.2
α -TACoPc@CNT	0.76	-4.97
β -TACoPc@CNT	0.65	-3.03

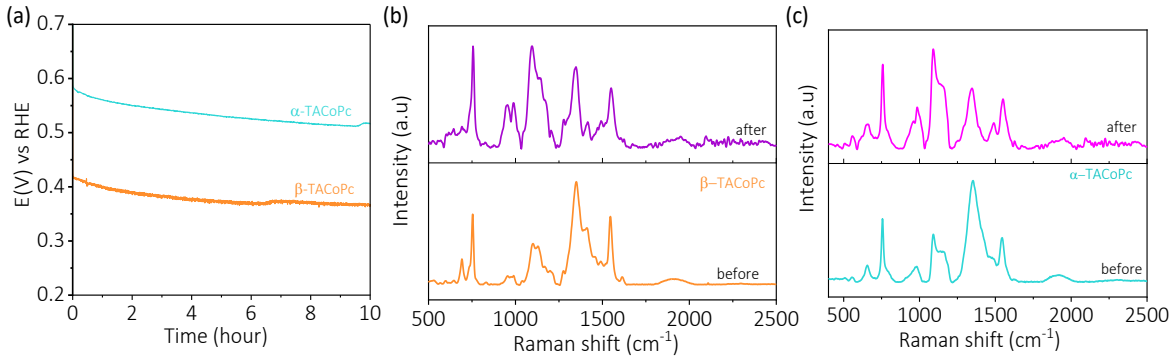

Figure S8: (a) Chrono-potentiometric analysis during ORR in oxygen saturated 0.1 M H_2SO_4 with α and β isomer molecules for 10 hours. (b) Raman spectra of the electrodes before and after long term stability tests in 0.1 M H_2SO_4 electrolyte.

Table S5: Parameters obtained from Fig. 3a.

Type of electrodes	HER	
	Onset Potential (V vs. RHE)	Current density @ -0.2 V vs RHE)
NPG	-0.19	-0.07 mA/cm^2
α -TACoPc@NPG	-0.14	-0.18 mA/cm^2
β - TACoPc@NPG	-0.07	-0.85 mA/cm^2

Table S6: Tafel slope extracted from Fig. 3c

Type of electrodes	Tafel Slope (mV/dec) (HER)
NPG	108
α -TACoPc@NPG	85
β - TACoPc@NPG	72

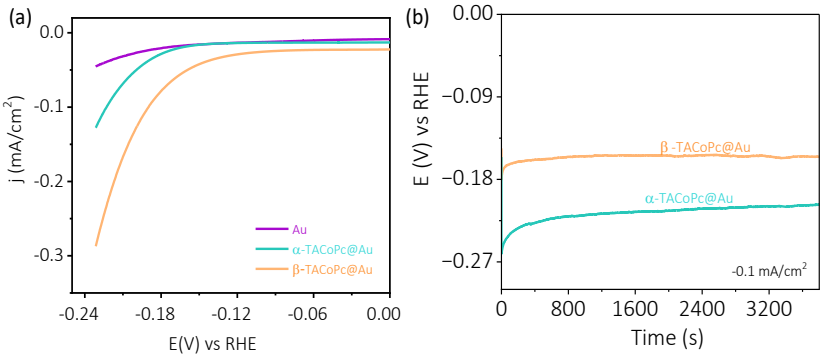

Figure S9: (a) Voltammograms of α -TACoPc and β- TACoPc modified (monolayers) Au electrodes with α and β TACoPc molecules in 0.1 M H_2SO_4 electrolyte at a scan rate of 5 mV/s. (b) Chronopotentiometric analysis at -0.1 mA/cm^2 for α-TACoPc and β-TACoPc molecules.

Table S7: Parameters calculated from Fig. S9.

Type of electrodes	HER	
	Onset Potential (V vs. RHE)	Current density @-0.2 V vs RHE
Au	-0.13	-0.02 mA/cm^2
α -TACoPc@Au	-0.16	-0.06 mA/cm^2
β -TACoPc@Au	-0.12	-0.15 mA/cm^2

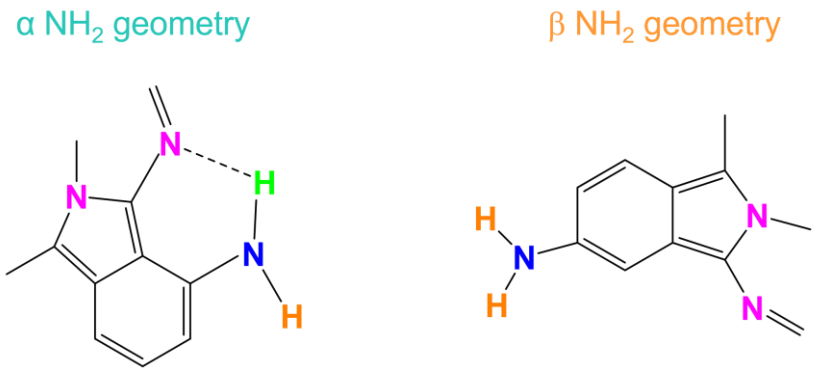

Scheme S1: Schematic representation illustrating intramolecular hydrogen bonding interactions in the α-NH_2 isomer, between the imine nitrogen and amine protons. Conversely, the β-NH_2 isomer demonstrates the absence of such interactions, attributed to the unfavorable positioning of hydrogen bonding groups.

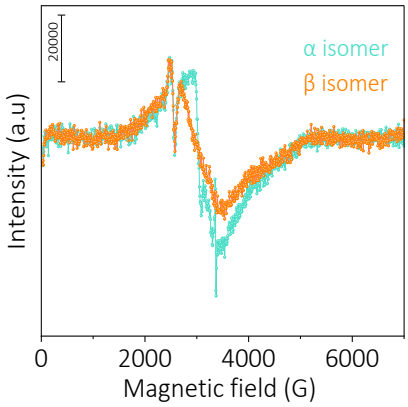

Figure S10: EPR spectra of α, β TACoPc collected at room temperature

Table S8: N1s Binding energy values for both isomeric molecules (extracted from Figs. 5c and 5d) N_1 (Co-N), N_2 (C=N, imine), N_3 (C-NH_2, amine)

Molecules	α -TACoPc			β -TACoPc		
	N_1	N_2	N_3	N_1	N_2	N_3
Pristine (eV)	398.9	399.4	401.2	398.8	399.2	400.9
Protonated (eV)	399.06	400.8	401.7	399.1	400.9	401.9
				N_1	N_2	N_3
Δ B.E [$\beta_{protonated}$ - $\alpha_{Protonated}$] (eV)				0.04	0.1	0.2

References:

[1] J. Alzeer, P. J. C. Roth, N. W. Luedtke, *Chem. Commun.* 2009, 1970–1971.

[2] R. Cao, R. Thapa, H. Kim, X. Xu, M. Gyu Kim, Q. Li, N. Park, M. Liu and J. Cho, *Nat. Commun.*, 2013, **4**, 2076

[3] R. Zhou, Y. Zheng, M. Jaroniec, S. Z. Qiao, *ACS Catal.* 2016, **6,** 4720–4728.

[4] P. Miedema, M. M. Van Schooneveld, R. Bogerd, T. Rocha, M. Hävecker, A. Knop-Gericke, F. De Groot, *J. Phys. Chem. C*, 2011, **115,** 25422–25428.